Jordan Journal of Civil Engineering, Volume **8**, No. **2**, **2014**

Wind Induced Pressure on 'E' Plan Shaped Tall Buildings

Biswarup Bhattacharyya [1)]***, Sujit K. Dalui*** [2)*] ***and Ashok K. Ahuja*** [3)]

[1)] Post-Graduate Student, Department of Civil Engineering, Bengal Engineering and Science University, Shibpur, Howrah, India.
[2)] Assistant Professor, Department of Civil Engineering, Bengal Engineering and Science University, Shibpur, Howrah, India.
[3)] Professor, Department of Civil Engineering, Indian Institute of Technology Roorkee, Roorkee, India.
* Corresponding Author: Howrah-711103, West Bengal, India.
E-Mail: sujit_dalui@rediffmail.com

ABSTRACT

The present study demonstrates the pressure distribution on various faces of 'E' plan shaped tall buildings under wind excitation. Experimental and analytical studies were carried out using wind angles varying from 0° to 180° with an interval of 30°. The experimental study was conducted by open circuit boundary layer wind tunnel; whereas the analytical study was conducted with Computational Fluid Dynamics (CFD) technique using ANSYS CFX software package using k-ε turbulence model. A rigid model (made of perspex sheet) was used for wind tunnel test with a model scale of 1:300. Mean pressure coefficients of all the faces are found for all wind incidence angles and pressure contours are plotted on all the surfaces for 0° wind angles. Mean pressure coefficients are also calculated by CFD technique and the results have a good agreement with experimental results. Also, pressure contours on all the faces for a 0° wind angle are plotted and the contours are almost similar to those of experimental investigation. The flow pattern around the building model is also shown to understand the variation of pressures on different faces for a particular wind angle.

KEYWORDS: Tall building, Wind tunnel test, Mean pressure coefficient, Computational Fluid Dynamics (CFD), Flow pattern.

INTRODUCTION

Wind engineering is best defined as the rational treatment of interactions between wind in the atmospheric boundary layer and man and his works on the surface of Earth. In the context of urbanization, land area is not expanding but population is increasing daily especially in cities. So, the requirement of high rise buildings is urgently needed. Such buildings may be of conventional shape in plan or may be irregular. Such irregular plan shape buildings are mostly efficient to utilize total land area. Wind load is mostly critical in case of high rise buildings. Pressure variation and force coefficient for such conventional plan shape buildings (i.e., rectangular, square… etc.) are given in relevant Indian code IS: 875 (Part-3):1987, Australian/New-Zealand code AS/NZS 1170.2: 2002, British code BS 6399-2: 1997, American code ASCE 7-02. However, these codes are totally silent about the pressure variation and force coefficient of unconventional or irregular plan shape buildings. Along wind action on building structures is more critical in case of conventional plan shape model, but irregular plan shape building may experience critical pressure

Accepted for Publication on 29/12/2013.

distribution on faces other than windward face.

Responses on irregular plan shaped buildings due to wind effects are estimated by Wind Tunnel test (experimental) procedure or Computational Fluid Dynamics (CFD) method (analytical). Some researchers in the field of wind engineering conducted work on irregular plan shape and high rise buildings. Gomes et al. (2005) investigated wind pressure distribution on the faces of 'L' and 'U' plan shape tall buildings by using wind tunnel test as well as computational fluid dynamics (CFD) method. Wind pressure distribution on various surfaces was observed to be different from square model. Mendis et al. (2007) provided an outline of advanced levels of design for wind loading for interference effects, along wind and across wind effects were considered. Wind Tunnel test and CFD analysis were conducted using ANSYS software. It was observed that the experimental and analytical results were in reliable limit (20%-25%). Also, Amin and Ahuja (2008) presented experimental results of pressure distribution on various faces of 'L' and 'T' plan shape tall buildings for various wind angles. It was noticed that pressure distribution largely depends on the plan shape of those tall buildings. Fu et al. (2008) presented field measurement results of boundary layer wind characteristics over typical open country and urban terrain for two super tall buildings. Full scale measurement results were compared with wind tunnel test data. It was noticed that results were within adequate limits (20%-25%). Tanaka et al. (2012) presented aerodynamic characteristics of different irregular plan shape tall buildings by wind tunnel test to evaluate the most effective structural shape under wind excitation. Results showed better aerodynamic behavior for 4-tappered model and setback model in along wind direction and helical model, cross opening models in cross wind direction in case of maximum mean overturning moment coefficients. But, in case of maximum fluctuating moment coefficients, corner modification model, tappered model and setback model showed better behavior for both along and cross wind directions. Local wind force coefficients of torsional moments were also small. Chakraborty et al. (2013) presented a comparative study of pressure on different faces of '+' plan shape tall building by computational fluid dynamics (CFD) method as well as by wind tunnel test for various wind angles. It was noticed that differences in pressure coefficients from CFD method and wind tunnel test were within the permissible limit. Pressure on some faces was changed due to interference effect of other faces. Chakraborty and Dalui (2013) presented a paper on a numerical study of pressure distribution on different faces of square plan shape tall buildings under 0°, 30° and 45° wind angles using ANSYS FLUENT software. Mean pressure coefficient for 0° wind angle was compared with IS 875 (Part 3):1987 (clause 6.2.2.1), the Indian standard code for calculating wind load on buildings, to validate the results. It was noticed that mean pressure coefficient on windward side face for 30° wind angle was almost zero. Also, the nature of pressure distribution was changed due to change in wind angles.

This paper presents the experimental study on 'E' plan shape tall buildings starting from 0° to 180° at an intermediate interval of 30°. The scale of the model is taken as 1:300. Experimental study was conducted by open circuit wind tunnel test. Analytical study was also carried out by Computational Fluid Dynamics (CFD) technique to validate and compare the results using ANSYS CFX software package.

The purpose of the study is to present pressure distribution on various faces of 'E' plan shape tall buildings for different angles of wind flow because these results are not incorporated in relevant codes. The wind flow pattern around the building is demonstrated. The variation of results between experimental and analytical study is also studied so that results can be incorporated in the relevant codes.

Experimental Setup

The experiments were conducted in an open circuit boundary layer wind tunnel (as shown in Fig. 1) at Wind Engineering Centre, Department of Civil

Engineering, Indian Institute of Technology Roorkee, India. Wind is continuously flowing through the tunnel by generating suction of a blower fan (125 HP). The wind tunnel cross-section is 2m (width) ×2 m (height) and the length of the wind tunnel is 38 m. A 6 m (width) × 6 m (height) square-holed honeycomb is located at the entrance of the wind tunnel to generate uniform flow throughout the wind tunnel. An elliptical effuse profile of 6m length with a contraction ratio of 9:5:1 is situated after the honeycomb to generate smooth wind flow throughout the tunnel. Vortex generators are given for developing boundary layer flow on the upstream side. The experiment was carried

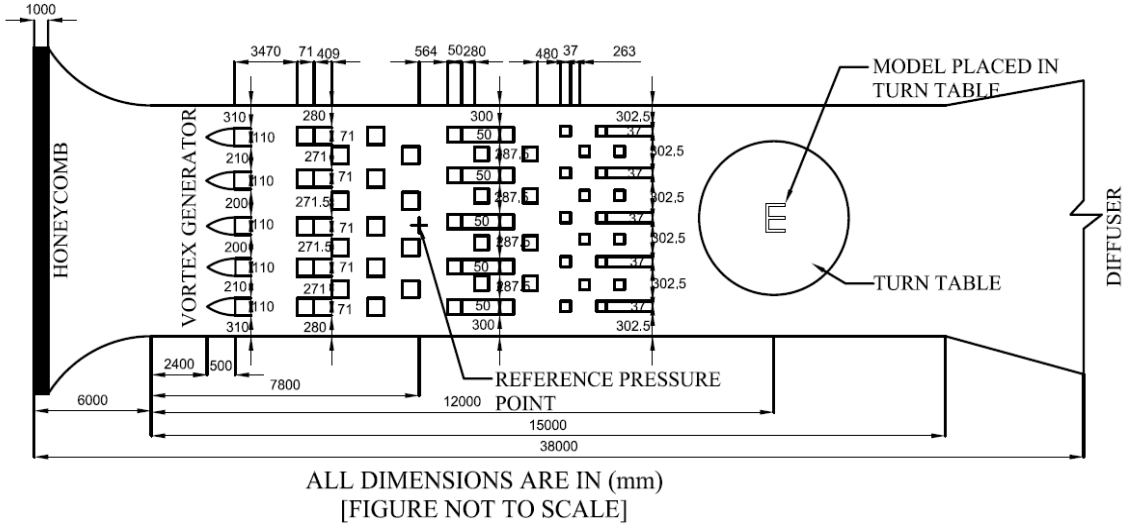

Figure (1): Model placed in wind tunnel (plan)

out as per terrain category II as given in Indian code IS 875 (Part 3)-1987. Terrain category was formed by providing square cubes of different sizes (7.1 cm, 5.0 cm and 3.7 cm) on the upstream side of the wind tunnel. A manual controlled turn table is located at 12m distance from the elliptical effuse to rotate pressure model in various angles. Pressure model is placed at the center of the turn table. Wind speed can be varied in the wind tunnel from 2 m/s to 20 m/s by controlling the dynodrive attached with diffuser or fan at the outlet of the wind tunnel. A pitot tube is located at a distance of 7.8 m from the elliptical effuse to measure wind flow velocity inside the wind tunnel and the reference pressure point is also located at the same distance. The wind tunnel is also machinated with a hot-wire anemometer and a monometer. A Pressure transducer is attached with the pressure points and the reference pressure point to measure pressures on the pressure tapping points which are processing through the barron instrument attached. 'Datataker' can take these pressure values from the barron instrument and force values from five component load balances and process these values to the computer which records these values and processes graphical and numerical values coming out from the experiments.

Overview of the Model

Pressure measurement model (as shown in Fig. 2) was made of a Perspex sheet having a thickness of 4mm. Different faces and isometric view of the model with detail dimensions are shown in Fig. 3. A total of 210 numbers of pressure tapping points (as shown in Fig. 4) were installed at five different heights of 10 mm, 100 mm, 250 mm, 400 mm and 490 mm from the

bottom on all the faces of the pressure measurement model. The pressure tapings were made of steel tubes with 1 mm internal diameter and were 15-20 mm long. These pressure tapings were installed in the model by drilling holes in each and every grid point. Pressure tapings were installed very close to the edges of the faces to study the changes of pressure variations due to separations of flow.

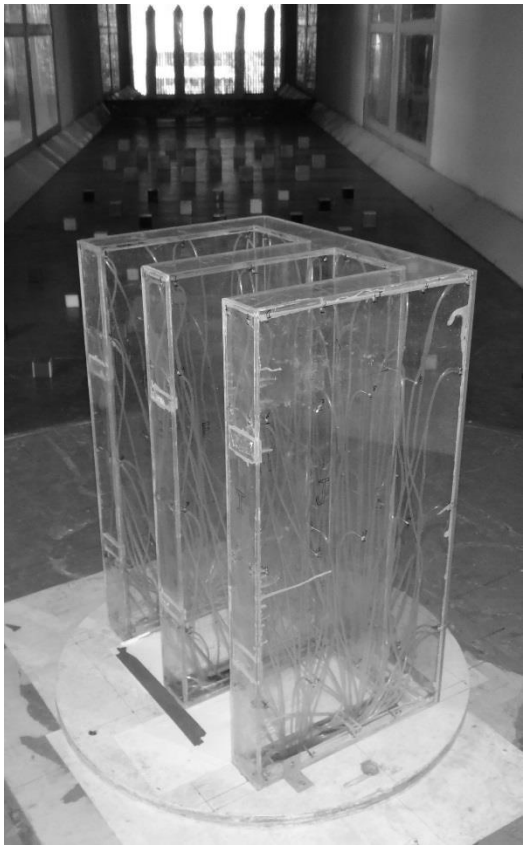

Figure (2): Pressure measurement model placed on turn table inside the wind tunnel

Boundary Condition

The velocity of wind in the wind tunnel was considered as 10 m/s and the turbulence intensity was 10% in the wind tunnel. Boundary layer flow was generated by vortex generator and cubic blocks placed in the upstream side of the wind tunnel. These cubic blocks were placed to simulate the experiment under terrain category II as given in IS 875 (Part 3):1987 (clause 5.3.2.1). The power law index (α) for the velocity profile inside the wind tunnel was 0.133. The pressure measurement model was placed in the center of the turn table, 12 m from the elliptical efuse in the upstream side. Free stream velocity was measured using a pitot tube during the experiment.

Numerical Study

Numerical study was carried out by Computational Fluid Dynamics (CFD) method using ANSYS CFX software. A two equation k-ε turbulence model was used for modelling to offer a good compromise between numerical effort and computational accuracy. K-ε model uses the gradient diffusion hypothesis to relate the Reynold stresses to the mean velocity gradients and turbulent viscosity. 'k' is the turbulence kinetic energy defined as the variance of fluctuations in velocity and 'ε' is the turbulence eddy dissipation (the rate at which the velocity fluctuation dissipates).

So, modified continuity and momentum equations after incorporating two new variables i.e., k and ε are given by equations 1 & 2.

$$\frac{\partial \rho}{\partial t} + \frac{\partial}{\partial \boldsymbol{x}_j}\left(\rho \boldsymbol{U}_j\right) = 0 \tag{1}$$

$$\frac{\partial \rho U_i}{\partial t} + \frac{\partial}{\partial x_j}\left(\rho U_i U_j\right) = -\frac{\partial p'}{\partial x_i} + \frac{\partial}{\partial x_j}\left[\mu_{eff}\left(\frac{\partial U_i}{\partial x_j} + \frac{\partial U_j}{\partial x_i}\right)\right] + S_M \tag{2}$$

where S_M is the sum of body forces, μ_{eff} is the effective viscosity accounting for turbulence and p' is the modified pressure. The k-ε model, like the zero equation model, is based on the eddy viscosity concept, so that:

$$\mu_{eff} = \mu + \mu_t \tag{3}$$

where μ_t is the turbulence viscosity. The k-ε model assumes that the turbulence viscosity is linked to

the turbulence kinetic energy and dissipation via the relation:

$$\mu_t = C_\mu \rho \frac{k^2}{\varepsilon} \quad (4)$$

where C_μ is a constantt.

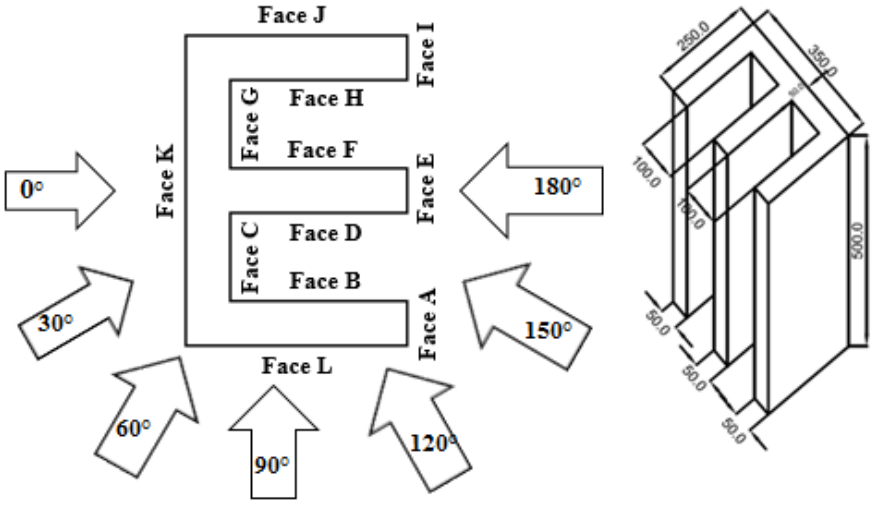

Figure (3): Different faces (showing different wind angles) and isometric view of the model

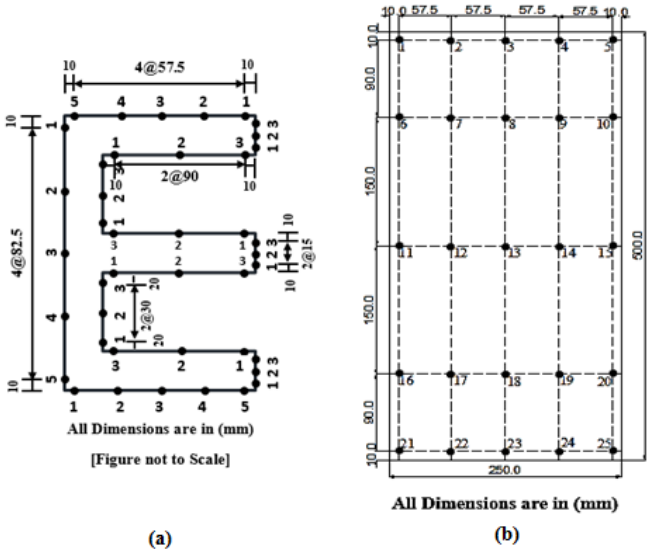

Figure (4): Pressure tapping points shown in (a) plan, (b) elevation

The values of k and ε come directly from the differential transport equations for the turbulence kinetic energy and turbulence dissipation rate:

$$\frac{\partial(\rho k)}{\partial t}+\frac{\partial}{\partial x_j}\left(\rho U_j k\right)=\frac{\partial}{\partial x_j}\left[\left(\mu+\frac{\mu_t}{\sigma_k}\right)\frac{\partial k}{\partial x_j}\right] + P_k-\rho\varepsilon+P_{kb} \quad (5)$$

$$\frac{\partial(\rho \varepsilon)}{\partial t}+\frac{\partial}{\partial x_j}\left(\rho U_j \varepsilon\right)=\frac{\partial}{\partial x_j}\left[\left(\mu+\frac{\mu_t}{\sigma_\varepsilon}\right)\frac{\partial \varepsilon}{\partial x_j}\right] + \frac{\varepsilon}{k}(C_{\varepsilon 1}P_k-C_{\varepsilon 2}\rho\varepsilon+C_{\varepsilon 1}P_{\varepsilon b}) \quad (6)$$

P_k is the turbulence production due to viscous forces, which is modeled using:

$$P_k=\mu_t\left(\frac{\partial U_i}{\partial x_j}+\frac{\partial U_j}{\partial x_i}\right)\frac{\partial U_i}{\partial x_j} - \frac{2}{3}\frac{\partial U_k}{\partial x_k}\left(3\mu_t\frac{\partial U_k}{\partial x_k}+\rho k\right) \quad (7)$$

C_μ is k-ε turbulence model constant with the value 0.09. $C_{\varepsilon 1}$, $C_{\varepsilon 2}$ are also k-ε turbulence model constants in ANSYS CFX with values of 1.44 and 1.92, respectively. σ_k is the turbulence model constant for k equation with the value of 1.0 and σ_ε is the turbulence model constant for ε equation with the value of 1.3. ρ is the density of air in ANSYS CFX taken as 1.224 kg/m^3. M and μ_t are dynamic and turbulent viscosity, respectively. The other notations have their usual meanings. The building was considered as bluff body in ANSYS CFX and the flow pattern around the building was studied. Turbulence intensity was considered as 10%.

Domain and Meshing

The domain size was taken as referred to by Revuz et al. (2012). The upstream side was taken as 5H from the face of the building, downstream side was taken as 15H from the face of the building, two side distance of the domain was taken as 5H from the face of the building and top clearance was taken as 5H from the top surface of the building. Such large size of downstream side helps in vortex generation in the leeward side of the flow and backflow of wind is also prevented. Multizone meshing and tetrahedron meshing were conducted throughout the domain with a hexagonal mesh and a tetrahedron mesh (Fig. 5), respectively. Finer hexegonal and tetrahedron meshes are very useful for generating uniform flow of wind throughout the domain so that seperation of flow is very smooth.

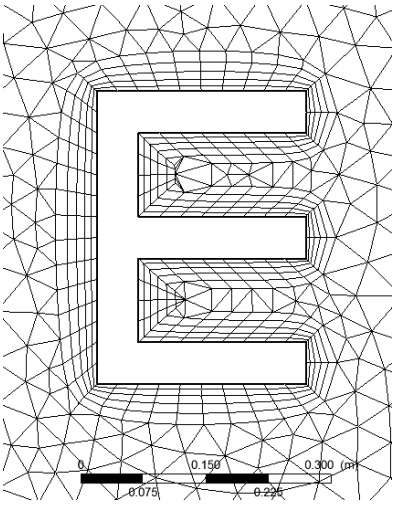

Figure (5): Mesh pattern around the building model (plan)

Flowing Criteria

The boundary conditions were taken as the same in the wind tunnel test such that the results found from the experiment can validate the results obtained from the numerical analysis.

Boundary layer wind flow near the windward side was generated in the inlet of the domain using power law:

$$\frac{U}{U_0}=\left(\frac{z}{z_0}\right)^\alpha \quad (8)$$

where U_0 is the basic wind speed taken as 10 m/s, Z_0 is the boundary layer height considered 1 m as the

wind tunnel and the power law index α was taken as 0.133. The velocity profile for the experimental and analytical investigation is shown in Fig. 6 which shows that the velocity profile is identical as experimental for the upper portion, but the lower portion found some discripancy due to the type of meshing and number of elements considered for the numerical model. The percentage of error may be reduced by changing the type of meshing and increasing the number of elements. For that purpose, high computational facilities are needed. However, for the present study the percentage of error (10.5%) is within the permissible limit. It seems that the analytical model is correct and the next steps can proceed. Relative pressure at the outlet was considered as 0 Pa. The velocity in all other directions was set to zero. Side surfaces and top surfaces of the domain were taken in free slip condition so that no shear stress should generate there; whereas all surfaces of the body were considered in no slip condition to measure the pressure contour accurately.

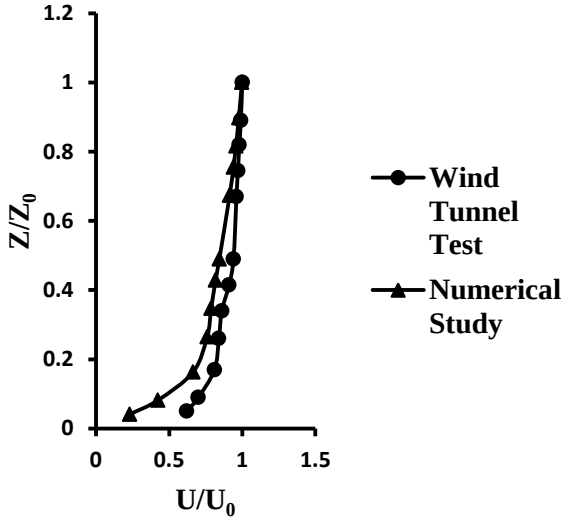

Figure (6): Comparison of velocity profile near test section

RESULTS AND DISCUSSION

1. Experimental Results

The values of pressure from each tapping point are found from the wind tunnel test. The mean pressure coefficient and pressure coefficient contour are plotted on all the faces taken from the wind tunnel test. Pressure coefficients of each pressure tapping point are found from the formula:

$$C_p = \frac{Pressure\ \ at\ any\ point(pa)}{0.6V_z^z} \qquad (9)$$

where V_z is the design wind speed in m/s which is considered as 10 m/s for this experiment. Also, the mean pressure coefficient of each surface is reported. Mean pressure coefficients of different surfaces are given in Table 1. Maximum positive mean pressure coefficient of 0.8 occurred on face E at a wind inclination angle of 180° and maximum negative mean pressure coefficient of -0.68 occurred on face A at a wind inclination angle of 90°. Maximum positive pressure occurs due to maximum wind energy which dissipiates on face E when wind flows at an angle of 180°. Also, the surface area of the face E is smaller compared to other faces and wind is hitting perpendicular to the surface. Maximum negative

pressure occurs on face A at an angle of 90° due to the seperation of wind flow and high suction force occurs on this face. Almost zero mean pressure coefficient occurs on face B (-0.01), G (0.04) at a wind flow angle of 120° and on face L (0.01) at a wind flow angle of 30°. In spite of zero mean pressure, the designer should be more careful about the structural design because almost equal portions or equal intensities of positive and negative pressure occurred on these faces. Generally, the structural elements of the faces of any building are designed by considering mean pressure coefficients, but it is better to consider node to node variation of pressure coefficient in critical condition. This will protect the building from wind desasters as well as being economically cheaper than mean pressure coefficient.

Pressure contours of all faces for 0° wind incidence angle are shown in Fig. 7. Pattern of pressure contour on face K is symmetrical about the vertical axis as the wind is hitting perpendicularly on the surface of the building. Also, the pressure contours of symmetrical faces about vertical axis are also similar. Maximum negative pressure (mean pressure coefficient of -0.51) for 0° angle of wind flow occurred on two side faces (face J and face L) due to high suction force in the wind flow seperation zone. Negative pressure occurred on all other faces of 'E' plan shape tall building.

Variations of pressure coefficient along the horizontal centerline, 100 mm below the topmost fiber of the building and 100 mm above the base of the building, are also plotted for detailed investigation. This will give the idealized pattern of pressure coefficient throughout all the faces of the 'E' plan shape tall building for various wind induced angles. The variations of pressure coefficinet along the horizontal centerline for all wind induced angles are shown in Fig. 8. This Figure shows that variations of pressure coefficinet for 0° and 180° are almost equal and opposite in nature bacause flow directions are also opposite. It is seen from Fig. 8 that pressure coefficient fluctuates from negative to positive with almost the same intensity from face A to face I at 120° angle of wind attack, so the mean pressure coefficients of these faces are almost zero or near to zero. This happened due to the formation of irregular vortex caused by the seperation of flow by the faces A, E and I. The effect of each seperation is influencing the other and the dynamic effect of wind is developing due to multi-seperation. Also, two vortices are generated in between the limbs of 'E' plan shape tall building.

The variations of pressure coefficient at the level of 100 mm from the top of the building and 100 mm from the bottom of the building are plotted in Fig. 9 and Fig. 10, respectively for 0° to 180° angles of wind flow. The variation of pressure coefficient is different from the previous one (horizontal centerline). It is observed that maximum positive pressure occurred on face E in the case of a wind induced angle of 180° at the level of 100 mm from the top of the building. Almost equal pressure is found from face A to face I for wind induced angles of 0°, 30° and 60° because of the rear side position with respect to the direction of wind flow.

Variation of pressure coefficient at the level of 100 mm from the base of the building (Fig. 10) is also noticeable and different from the previous two cases. Almost equal negative pressure occurred on face A to face I for wind incidence angles of 0° to 60°. Similarly, almost the same positive pressure is noticed on face A to face I for wind induced angles of 150° and 180°. But, a large variation is observed for wind induced angles of 90° and 120° due to change in the direction of wind flow. The seperation of wind flow is also different for wind induced angles of 90° and 120°. It is noticed from all three plots that the variations of pressure coefficient on face J for all wind induced angles in all three levels are negative in nature due to the formation of vortex or seperation of flow.

Pressure coefficient variations of some faces along vertical centerline for all wind incidence angles of wind flow are shown in Fig. 11. It is noticed from the Figure that the variation of pressure coefficient on faces A, B and D for 0°, 30° and 60° wind incidence angles is almost similar. Similarly, pressure variation on face K at 120°, 150° and 180° angle of wind flow are almost

similar. The variation of pressure coefficients along the vertical centerline on faces B and D is almost equal for all wind incidence angles. Similarities occurred due to equal and opposite faces and wind flow equally affected the faces.

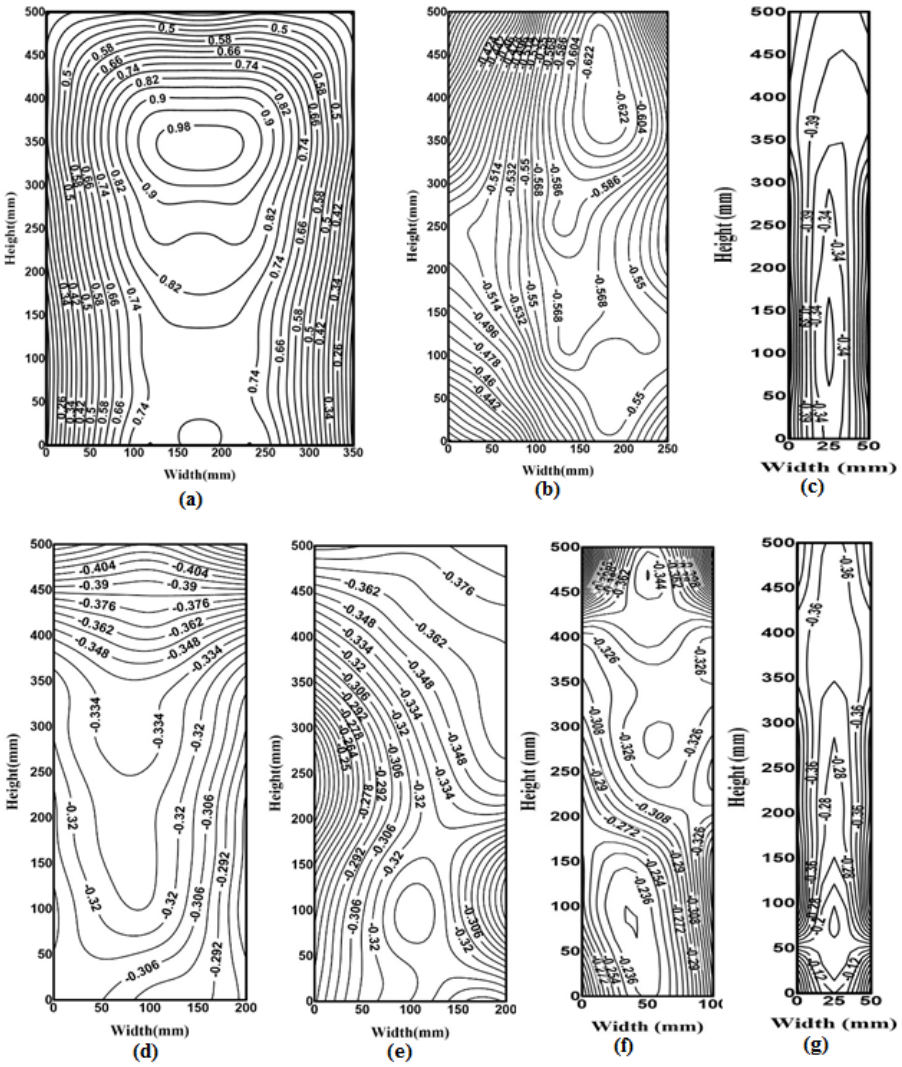

Figure (7): Pressure contour on different surfaces of the model (Experimental Study/ Wind Tunnel test); (a) Face K, (b) Faces J & L, (c) Faces A & I, (d) Faces B &H, (e) Faces D & F, (f) Faces C & G, (g) Face E

2. Numerical Results

Mean pressure coefficients of all the faces are also found from numerical analysis using ANSYS CFX software package with k-ε turbulence model. The mean pressure coefficients of some of the faces for various angles of wind flow are given in Table 2 with experimental results to validate the numerical results. Pressure contours of all faces for 0° wind incidence angle are shown in Fig. 12.

From Table 2, it is seen that mean pressure coefficients calculated by numerical methods are within the reliable limit with respect to the

experimental values. Highest percentage of error occurred on face J with 15.15% for 120° wind angle whereas minimum percentage of error occurred on face L with 1% for 30° wind angle. Mean pressure coefficients of other surfaces are also given for different wind angles in Table 2 and these values are almost submerging with the experimental values.

Pressure contour plots on all faces for 0° wind angle are also similar to those of experimental plots. Pressure contours for different faces compared with experimental results. Mean pressure coefficients of these surfaces are also within the reliable limit with respect to the experimental results.

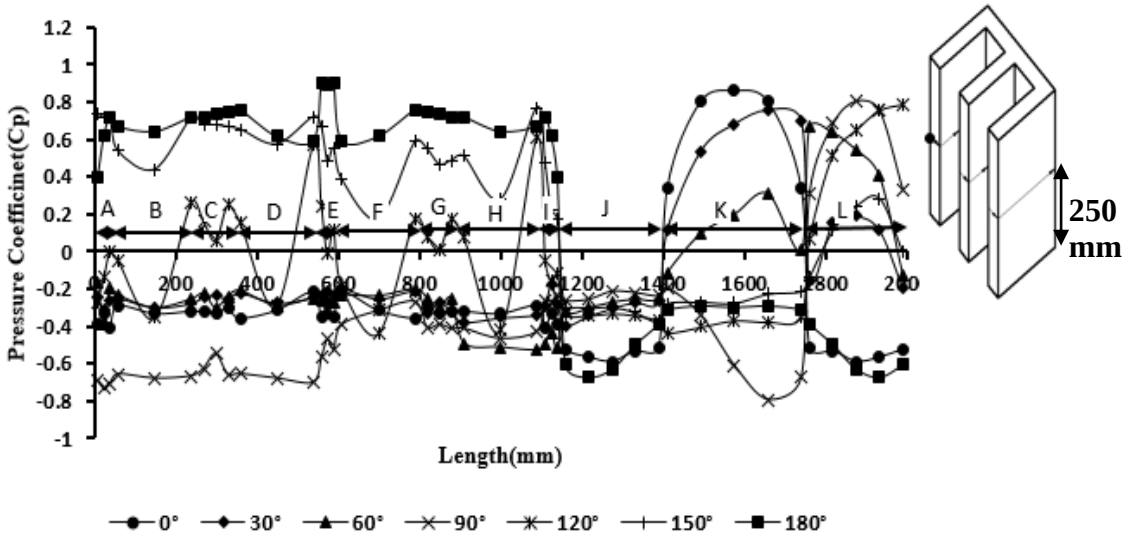

Figure (8): Variation of pressure coefficients along horizontal centerline

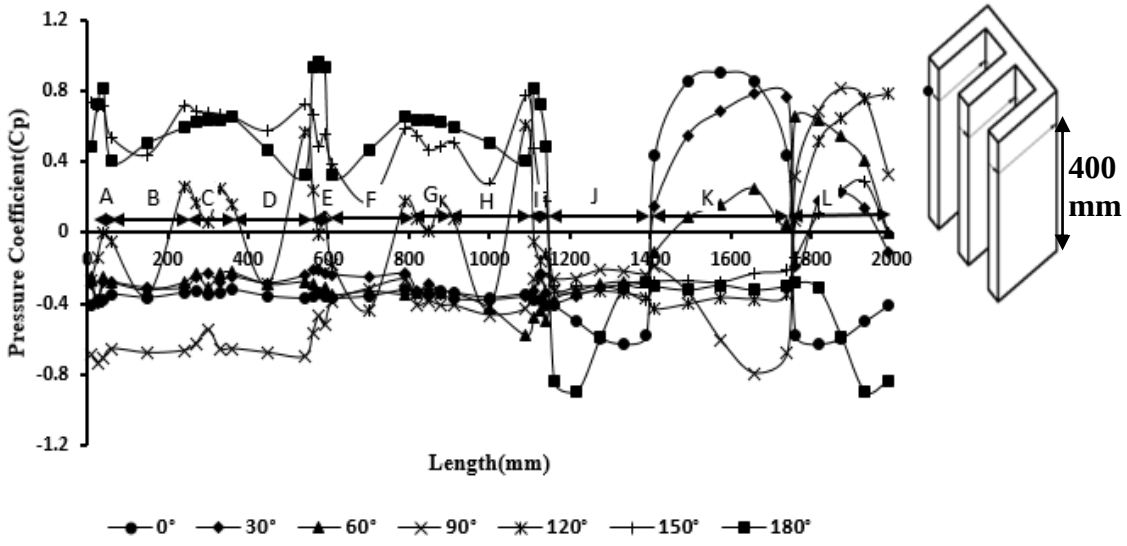

Figure (9): Variation of pressure coefficients at 100 mm below top of the building model

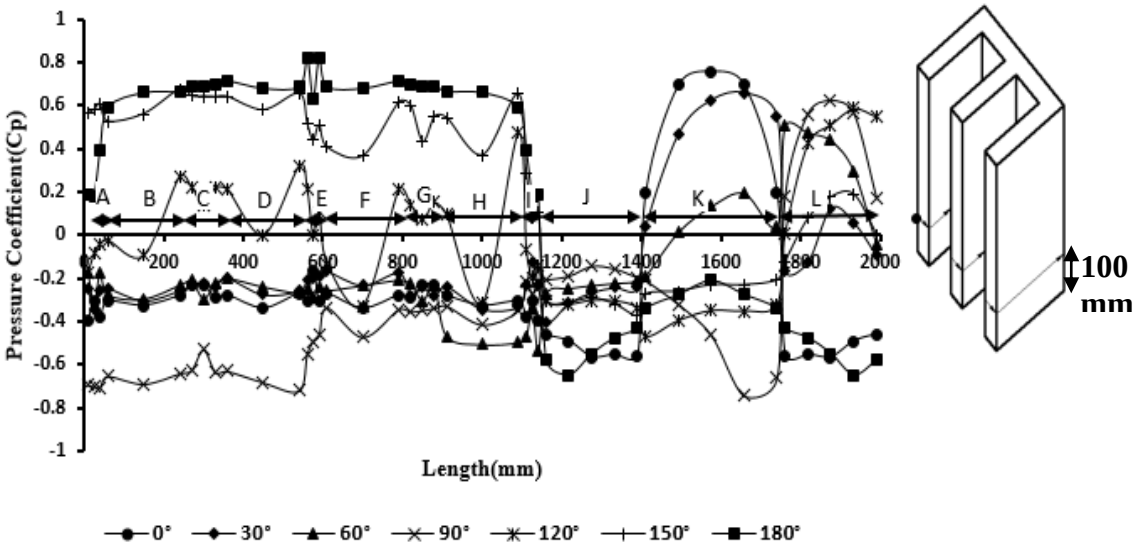

Figure (10): Variation of pressure coefficients at 100 mm above base of the building model

Table 1. Mean pressure coefficients of all surfaces of 'E' plan shape tall building for various wind angles

Face	Angle of Wind Flow						
	0°	30°	60°	90°	120°	150°	180°
A	-0.38	-0.28	-0.26	-0.68	-0.1	0.62	0.39
B	-0.34	-0.29	-0.28	-0.67	-0.01	0.43	0.47
C	-0.31	-0.25	-0.26	-0.61	0.13	0.51	0.55
D	-0.33	-0.25	-0.25	-0.67	0.13	0.51	0.53
E	-0.28	-0.22	-0.28	-0.47	0.08	0.51	0.8
F	-0.33	-0.22	-0.27	-0.36	-0.13	0.31	0.53
G	-0.31	-0.3	-0.28	-0.38	0.04	0.39	0.55
H	-0.34	-0.34	-0.41	-0.37	0.07	0.41	0.47
I	-0.38	-0.27	-0.46	-0.24	-0.15	0.23	0.39
J	-0.51	-0.32	-0.27	-0.21	-0.33	-0.33	-0.57
K	0.55	0.48	0.03	-0.49	-0.38	-0.26	-0.3
L	-0.51	0.01	0.36	0.44	0.45	0.11	-0.57

Numerically Predicted Wind Flow

Flow pattern around the building is predicted by numerical solution. The wind flow patterns for various angles are different. Patterns of pressure distribution on different faces are predicted at a particular wind flow direction. Flow pattern for a wind incidence angle of 60° is shown in Fig. 13. Plan view and elevation view of flow around the model are shown.

In the plan view, two vortices are formed in the rear side or in the outlet region of the domain, but the vortices are not similar in nature. So, the pressure distribution is also not similar on the faces. Also, two small vortices are formed in between the limbs of 'E' plan shape tall building. Negative pressure distribution

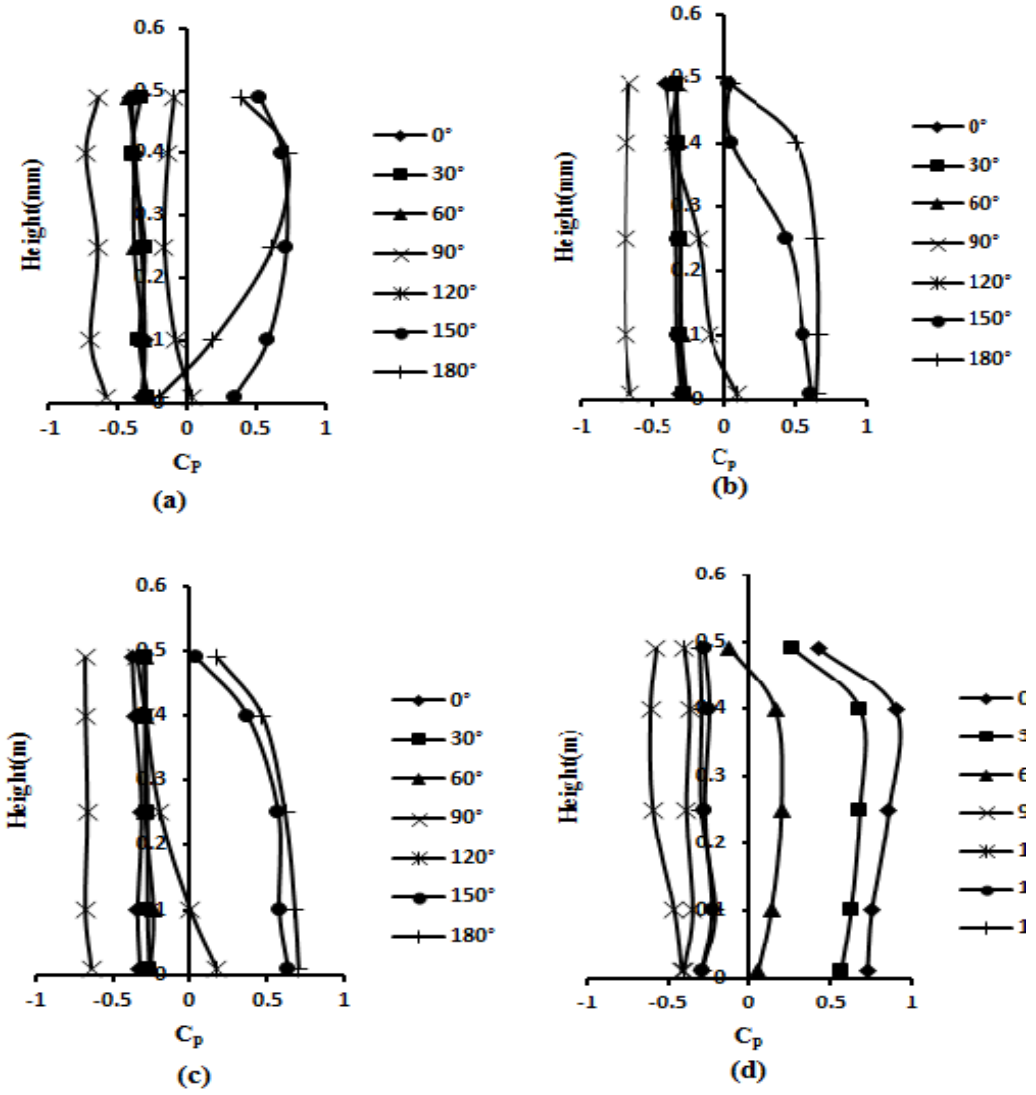

Figure (11): Variation of pressure coefficients along vertical centerline of (a) Face A, (b) Face B, (c) Face D, (d) Face K

Table 2. Comparison of mean pressure coefficients between experimental and analytical studies

Angle of wind flow	Face	Mean Surface Pressure Coefficient			Change in magnitude w. r. t. (experimental)	Remarks
		Experimental Result	Numerical Result			
0°	**K**	0.55	0.54		2%(Decrease)	Results are within acceptable limits
30°	**L**	0.01	0.00		1%(Decrease)	
60°	**H**	-0.41	-0.37		9.75%(Decrease)	
90°	**E**	-0.47	-0.4		14.89%(Decrease)	
120°	**J**	-0.33	-0.28		15.15%(Decrease)	
150°	**G**	0.39	0.34		12.82%(Decrease)	
180°		**B & H**	0.47	0.50	6.38%(Increase)	

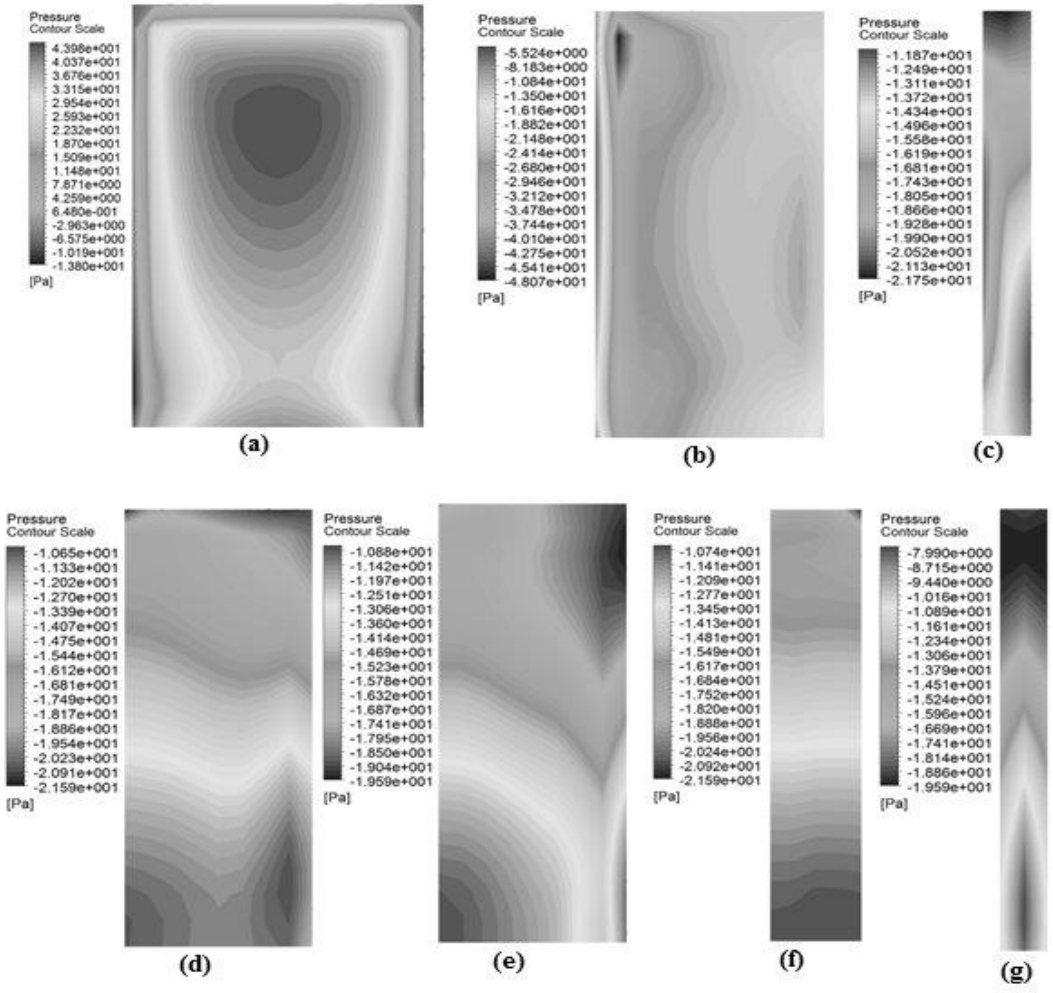

Figure (12): Pressure contour on different surfaces of the model (Numerical Study/ k-ε model); (a) Face K, (b) Faces J & L, (c) Faces A & I, (d) Faces B &H, (e) Faces D & F, (f) Faces C & G, (g) Face E

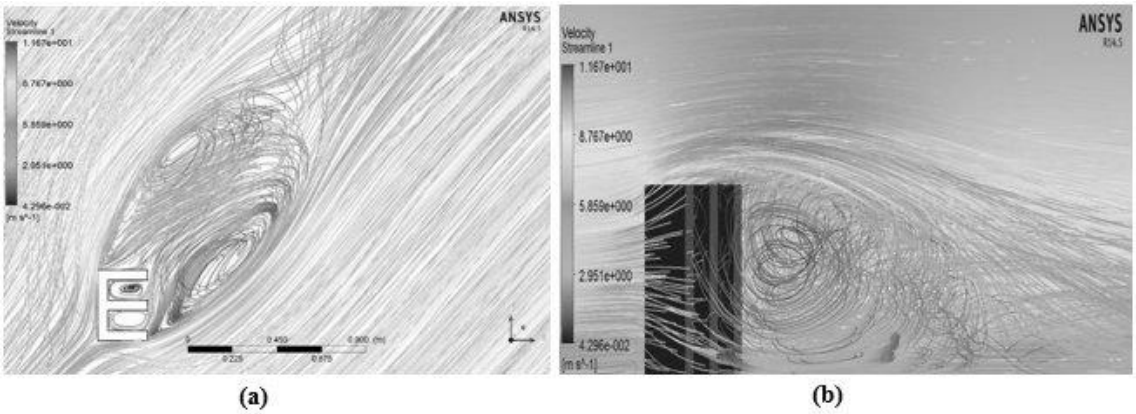

Figure (13): Flow pattern around the building model; (a) plan, (b) elevation

occurred on these faces due to suction force acting at the vortices. Also, negative pressure occurred on face A and face J due to seperation of wind flow and high suction force acting at the edges by the seperation of wind flow. Face K and face L experienced direct wind force, so positive pressure occurred on these faces. The intensity of formation of vortices is gradually increasing in nature from bottom to top.

CONCLUSIONS

This paper described the variation of pressure on all the surfaces of 'E' plan shape tall building for wind angle varying from 0° to 180° at an interval of 30°. Both experimental and numerical studies have been conducted. The wind flow pattern around the building model has been also presented using software package ANSYS CFX. Key features observed from the study are discussed below.

- Maximum positive mean pressure coefficient (0.8) occurred on face E for 180° wind angle and maximum negative mean pressure coefficient (-0.68) occurred on face A for 90° wind angle.
- Variations of pressure coefficient along horizontal and vertical centerline have been also studied. Fluctuation of pressure coefficient from face A to face I varies from negative to positive with almost equal intensity, so almost zero mean pressure coefficients occurred on these faces. Variations of pressure coefficient on faces A, B and D are almost equal for 0°, 30° and 60° wind angles through the vertical centerline.
- Variation of pressure coefficient at the level of 100 mm above base and 100 mm below top of the building model was also studied. The pressure variation was different from that of horizontal centerline. Almost equal pressure coefficients occurred on face A to face I for 0° to 60° wind angle in both cases. But, maximum positive pressure occurred on face E at the level of 100 mm from the top of the building model. Pressure variations on face J at all three horizontal levels are negative for all wind incidence angles.
- Mean pressure coefficients calculated numerically using k-ε turbulence model (Table 2) were almost the same as the experimental results. The differences are within the reliable limit.
- Patterns of pressure distribution on all faces for all wind incidence angles are predicted through observing wind flow patterns around the building model.
- Numerical results may vary for different meshing properties and different meshing sizes. Implementation of finer meshing sizes may be helpful to minimize the errors, but it also needs high mechanical configuration.

ACKNOWLEDGEMENT

The financial support of the experimental study by Department of Science & Technology (DST), India is greatly appreciated. The work was fully supported by Wind Engineering Center (WEC) of IIT Roorkee, Roorkee, India.

REFERENCES

Amin, J. A., and Ahuja, A. K. (2012). "Wind-Induced Mean Interference Effects Between Two Closed Spaced Buildings." KSCE Journal of Civil Engineering, 16 (1), 119-131.

ANSYS 14.5, "ANSYS, Inc.", www.ansys.com

ASCE 7-02. (2002). Minimum Design Loads for Buildings and Other Structures, American Society of Civil Engineering, ASCE Standard, Second Edition, Reston, Virginia.

AS/NZS 1170.2: 2002. (2002). Structural Design Action, Part 2: Wind Actions, Australian/ New-Zealand Standard, Sydney, Wellington.

BS 6399-2: 1997. (1997). Loading for Buildings- Part 2: Code of Practice for Wind Loads, British Standard, London, UK.

Chakraborty, S., Dalui, S. K., and Ahuja, A. K. (2013). "Experimental and Numerical Study of Surface Pressure on '+' Plan Shape Tall Building." International Journal of Construction Materials and Structures, 1 (1), 45-58.

Chakraborty, S., and Dalui, S. K. (2013). "Numerical Study of Surface Pressure on Square Plan Shape Tall Building." Symposium on Sustainable Infrastructure Development (SID), February 8th to 9th, 252-258, IIT Bhubaneswar, Bhubaneswar, Odisha, India.

Fu, J. Y., Li, Q. S., Wu, J. R., Xiao, Y. Q., and Song, L. L. (2008). "Field Measurements of Boundary Layer Wind Characteristics and Wind-induced Responses of Super-tall Buildings." Journal of Wind Engineering and Industrial Aerodynamics, 96 (8-9), 1332-1358.

Gomes, M. G., Rodrigues, A. M., and Mendes, P. (2005). "Experimental and Numerical Study of Wind Pressures on Irregular Plan Shapes." Journal of Wind Engineering and Industrial Aerodynamics, 93 (10), 741-756.

IS: 875 (Part 3). (1987). Indian Standard Code of Practice for Design Wind Load on Buildings and Structures, Second Revision, New Delhi, India.

Mendis, P., Ngo, T., Haritos, N., Hira, A., Samali, B., and Cheung, J. (2007). "Wind Loading on Tall Buildings." Electronic Journal of Structural Engineering, EJSE Special Issue: Loading on Structures, 41-54.

Revuz, J., Hargreaves, D. M., and Owen, J. S. (2012). "On the Domain Size for the Steady State CFD Modelling of a Tall Building." Wind and Structures, 15 (4), 313-329.

Tanaka, H., Tamura, Y., Ohtake, K., Nakai, M., and Kim, Y. C. (2012). "Experimental Investigation of Aerodynamic Forces and Wind Pressures Acting on Tall Buildings with Various Unconventional Configurations." Journal of Wind Engineering and Industrial Aerodynamics, 107-108, 179-191.